

Direct evidence of two-step disordering of the vortex lattice in a 3 dimensional superconductor, $\text{Co}_{0.0075}\text{NbSe}_2$

Somesh Chandra Ganguli^a, Garima Saraswat^a, Rini Ganguly^a, Harkirat Singh^a, Vivas Bagwe^a, Parasharam Shirage^b, Arumugam Thamizhavel^a and Pratap Raychaudhuri^a

^a *Tata Institute of Fundamental Research, Homi Bhabha Road, Colaba, Mumbai 400005, India.*

^b *Indian Institute of Technology Indore, IET-DAVV Campus, Khandwa Road, Indore 452017, India.*

The vortex lattice in a Type II superconductor provides a rich playground to investigate the order-disorder transition in a periodic medium in the presence of random pinning. Here, using scanning tunnelling spectroscopy in a weakly pinned $\text{Co}_{0.0075}\text{NbSe}_2$ single crystal, we show the existence of a hexatic state between the quasi-long range ordered Bragg glass and the fully disordered vortex glass state. By step by step imaging of the vortex lattice as a function of magnetic field at 350 mK, we show that the equilibrium Bragg glass realised at low magnetic field first transforms into a hexatic glass through the proliferation of dislocations. At a higher field, the dislocations dissociate into isolated disclination giving rise to an amorphous vortex glass. Our results show that while the vortex lattice in a 3D superconductor follows the same two-step route to disordering as that of a 2 dimensional hexagonal crystal, the presence of a random pinning potential gives rise to a variety of additional non-equilibrium states, which can be accessed through different thermomagnetic cycling.

Introduction

The competition between interaction and random pinning in a periodic medium connects to some of the most interesting problems in modern condensed matter physics. The vortex lattice (VL) in a Type II superconductor, where interactions favour the ordering of the vortices in a hexagonal Abrikosov lattice and crystalline imperfections provide a random background which can pin these vortices at random sites, has long been identified as a model system to study the order-disorder transition in the presence of random pinning^{1,2,3}. Over the past two decades, there have been intense efforts to understand the precise nature of the order-disorder transition with temperature or magnetic field. It is generally accepted that in a clean system the hexagonal VL realised at low temperature and magnetic field, can melt into a vortex liquid⁴ at a characteristic temperature (T) and magnetic field (H). Random pinning, significantly complicates this scenario. It has been argued that since the system can no longer sustain true long-range order, both the ordered and the disordered state become glassy in nature^{5,6}, characterised by different degree of positional and orientational order. In addition, the VL can exist in a variety of non-equilibrium metastable states^{7,8}, depending on the thermomagnetic history of the sample.

The order-disorder transition of a hexagonal lattice can follow two different routes. The first route is a direct transition from an ordered state to a disordered state through a first order phase transition. The second route is through two continuous transitions⁹, originally proposed by Berezinskii¹⁰, Kosterlitz and Thouless¹¹ and further refined by Halperin¹², Nelson and Young¹³ (BKTHNY) to explain the order-disorder transition in 2 dimensional (2D) systems. In this case, first, dislocations proliferate in the hexagonal lattice creating an intermediate state between the ordered and the disordered state, called the hexatic state, which has no long-range positional order but retains the 6-fold orientational order of the crystal. Subsequently, the disclination pairs that form the dislocations dissociate to form a

completely disordered state with no positional or orientational order¹⁴. In vortex lattices, evidence of topological defect mediated disordering has been reported^{15,16,17} in superconducting thin films.

In 3-dimensional (3D) superconductors, the order disorder transition has been extensively studied through bulk measurements, such as critical current¹⁸, ac susceptibility^{19,20} and dc magnetisation^{21,22}. These studies rely on the fact that in the presence of random pinning centres, the VL gets more strongly pinned to the crystal lattice as the perfect hexagonal order is relaxed²³. The order-disorder transition thus manifests as sudden non-monotonic enhancement of bulk pinning²⁴, and consequently of the critical current and the diamagnetic response in ac susceptibility measurements below the upper critical field (H_{c2}). This effect, known as the “peak effect”, has been a central theme of many studies and its evolution with magnetic field (H) and temperature (T) has been widely used to obtain the order-disorder transition line in the H - T parameter space. It has been argued that though the transition gets significantly broadened in the presence of random pinning, it still retains a first order character^{25,26,27,28,29}.

Here, using real space imaging through scanning tunnelling spectroscopy (STS) at 350 mK in a weakly pinned $\text{Co}_{0.0075}\text{NbSe}_2$ single crystal, we demonstrate the existence of a hexatic state between the equilibrium quasi-long range ordered Bragg glass⁵ state at low magnetic fields and the fully disordered isotropic vortex glass⁶ at high fields. Our study differs from earlier STS imaging studies^{17,30,31} in the fact that each VL image consists of several hundred to a thousand vortices, which allows us to accurately quantify the positional and orientational order, in each of these states. Comparing with the bulk pinning response of the crystal measured from ac susceptibility, we show that the VL lattice disorders through two continuous transitions across the peak effect rather than a first order phase transition.

Results

A. Bulk pinning properties

Fig.1 shows the bulk pinning response, measured from the real part of the ac susceptibility (χ'), of the VL at 350 mK when the sample is cycled through different thermomagnetic histories. We concentrate on two primary states: The zero field cooled (ZFC) state where the magnetic field is ramped up after the sample is cooled in zero magnetic field, and the field cooled (FC) state where the sample is cooled in the presence of magnetic field from a temperature, $T > T_c$. The χ' - H for the ZFC state (red line) is obtained while ramping up the magnetic field after cooling the sample to 350 mK in zero magnetic field. The “peak effect” manifests as a sudden increase in the diamagnetic response (inverted peak) between 16 kOe (H_p^{on}) to 25 kOe (H_p) after which χ' monotonically increases up to $H_{c2} \sim 38$ kOe. When the magnetic field is ramped down after reaching a value $H > H_{c2}$ (black line, henceforth referred as the ramp down branch), we observe a hysteresis starting below H_p and extending well below H_p^{on} . Similar hysteresis, earlier observed from magnetisation measurements has been attributed to the supercooling of the high-field VL state^{29,21}. The magnetic field dependence of the FC state is obtained by measuring χ' for the sample after it is cooled to 350 mK in a given field from 7 K (solid squares) and joining the loci of these points (dashed line). The FC state has a stronger diamagnetic response compared to ZFC and merges with the ZFC state for $H > 32$ kOe. When the magnetic field is ramped up or ramped down from the pristine FC state, χ' merges with the ZFC branch or the ramp down branch respectively, signifying that it is a non-equilibrium disordered state which undergoes a dynamic transition to a more ordered state²⁰ when the magnetic field is perturbed. In contrast, χ' for the ZFC state is reversible with magnetic field cycling up to H_p^{on} , suggesting that it is the equilibrium state of the system.

B. Evolution of the VL with magnetic field using space imaging

First, we follow on the VL configuration at 350 mK along the ZFC ramp up branch. Figure 2 (a)-(f) show the VL configuration for 6 representative fields along with the Fourier transforms for each image. While all images were acquired over $1\text{ }\mu\text{m} \times 1\text{ }\mu\text{m}$ area, for visual clarity the real space images are zoomed to show an area containing approximately 600 vortices. We identify 3 distinct regimes. For $H < H_p^{on}$, the VL lattice is hexagonally ordered and free from topological defects. Between $H_p^{on} < H \leq H_p$ dislocations (pairs of nearest neighbor points with 5-fold and 7-fold coordination) gradually proliferate in the system. Since dislocations destroy the positional order but do not destroy the long-range orientational order, this state can be characterized as a hexatic glass. For $H > H_p$ the disinclinations (isolated lattice points with 5-fold or 7-seven fold coordination) proliferate in the system driving the VL into an isotropic vortex glass. We observe significant range of phase coexistence³², where both large patches with dislocations coexist with isolated disinclinations. The Fourier transforms of the images show 6 spots for $H < H_p$. Above H_p , the Fourier transforms shows a ring characteristic of an isotropic disordered state.

Further confirmation of this sequence of disordering is obtained from the orientational and positional correlation functions, $G_6(\bar{r})$ and $G_{\bar{K}}(\bar{r})$, which measure the degree of misalignment and the relative displacement between two vortices separated by distance r respectively, with respect to the lattice vectors of an ideal hexagonal lattice. The orientational correlation function is defined as, $G_6(r) = \langle \cos 6(\theta(0) - \theta(\bar{r})) \rangle$, where $\theta(\bar{r}) - \theta(0)$ is the angle between the bond located at origin and the bond located at position \bar{r} . We calculate $G_6(r)$ by evaluating the average, $\frac{1}{n(r)} \sum_r^{r+\delta r} \cos 6(\theta(0) - \theta(\bar{r}))$, over a circular shell containing $n(r)$ bonds

at distance r from the origin, and further averaging over this quantity calculated by shifting the origin over the mid-point of each of the bonds in the lattice. The spatial correlation function, $G_{\bar{K}}(r) = \langle \cos \bar{K} \cdot \bar{r} \rangle$, (where \mathbf{r} is the position of the vortex and \mathbf{K} is the reciprocal lattice vector obtained from the Fourier transform) is calculated from the position of the vortices using a similar averaging procedure. For an ideal hexagonal lattice both $G_6(r)$ and $G_{\bar{K}}(r)$ are 1 for all values of r .

Figure 3(a) and 3(b) show the $G_{\bar{K}}(r)$ (averaged over the 3 principal \mathbf{K} directions) and $G_6(r)$ plotted as a function of r/a_0 (where a_0 is the average lattice constant) for different fields. At 10 kOe and 15 kOe, within our field of view, $G_6(r)$ decreases slightly from 1 and saturates to a constant value of ~ 0.93 and ~ 0.91 respectively after 2.5 lattice constants, while $G_{\bar{K}}(r)$ decays slowly with r . While we cannot unambiguously establish the functional form for the decay of $G_{\bar{K}}(r)$ at these fields due to the limited field of view, the slow decay in $G_{\bar{K}}(r)$ is qualitatively consistent with the quasi long-range order expected for a Bragg glass. Between 20 kOe and 25 kOe, $G_{\bar{K}}(r) \propto e^{-r/\xi_p}$ (ξ_p is the decay length of positional order) whereas $G_6(r)$ decays as a power law (Fig. 3(c) and 3(d)). This signals a complete destruction of long-range positional order but the persistence of a quasi long-range orientational order, characteristic of the hexatic state. Above 26 kOe, $G_6(r) \propto e^{-r/\xi_{or}}$ (ξ_{or} is the decay length of orientational order), giving rise to regular amorphous vortex glass state with no long-range positional or orientational order (Fig. 3(e)). It is however important to note that both of these transitions are considerably broadened: Between H_p^{on} and H_p , ξ_p decreases gradually and above H_p , ξ_{or} decreases gradually up to 3 T (Fig. 3(f)).

We now focus on the origin of the hysteresis observed between the ZFC state and the ramp down branch in χ' - H measurements. We show the VL images for the ramp down branch

at two fields: At 25 kOe (Fig. 4(b)) which is just below H_p ; and at 15 kOe (Fig. 4(a)) which is just below H_p^{on} , but much higher than the peak in χ' observed in the ramp down branch. At 25 kOe, we observe one disinclination pair (in 1200 vortices) within the field of view. However, analysis of the correlation functions show that $G_6(r)$ decays as a power-law (Fig. 4(e)) and $G_{\bar{K}}(r)$ decays exponentially (Fig. 4 (f)), characteristic of a hexatic glass. At 15 kOe, the VL is in a Bragg glass state (Fig. 4(c)-(d)), though $G_6(r)$ and $G_{\bar{K}}(r)$ are smaller than the corresponding ZFC state, showing that the ramp down branch is more disordered. However, our data does not provide any evidence of supercooled vortex glass state below H_p or the hexatic state below H_p^{on} in the ramp down branch.

We can now follow the magnetic field evolution of the FC state (Fig. 5). The FC state show a hexatic glass at 10 kOe (not shown) and 15 kOe, and a vortex glass above 20 kOe. The FC hexatic state is however extremely unstable. This is readily seen by applying a small magnetic pulse (by ramping up the field by a small amount and ramping back), which annihilates the dislocations in the hexatic state (Fig. 6). While many of the dislocations get annihilated with a pulse of 0.3 kOe, a larger pulse of 0.9 kOe annihilates all the dislocations in the FC hexatic state (at 1.5 T) causing a dynamic transition to a Bragg glass. It is interesting to note that metastability of the VL persists even in the fully disordered state above H_p where both ZFC and FC states are vortex glass. The FC state is more disordered with a faster decay in $G_6(r)$, and consequently more strongly pinned than the ZFC state.

Discussion

In BKTHNY theory^{10,11,12,13}, the hexatic state appears as an intermediate oriented fluid between a fully ordered 2-D solid and an isotropic liquid. Our measurements show that disordering of a weakly pinned VL in a 3D crystal follows a similar sequence, but with some

important differences. First, true long range order is no longer sustained in the presence of pinning. Instead, the system transforms into a Bragg glass, with nearly perfect orientational order, but a slowly decaying positional order. Secondly, the presence of random pinning prevents from establishing a fluid state. Instead, both the hexatic and the fully disordered state have quenched (or very slow) relaxation dynamics, characteristic of a glassy state. The quenched dynamics also broadens the transitions, and manifest as a slow decrease of ξ_p and ξ_{or} in the hexatic state and vortex glass state respectively. A natural consequence of the glassy nature is that the system can be stabilised in large number of non-equilibrium states such as the FC hexatic state below H_p^{on} and the FC vortex glass state below H_p .

The absence of supercooling of either the vortex glass state or the hexatic state below the corresponding critical fields H_p and H_p^{on} in the ramp down branch is consistent with BKT theory where both transitions are expected to be continuous. While our measurements cannot preclude the possibility of supercooling over a very small range of magnetic field, this would not explain the large magnetic range over which the hysteresis is observed in χ - H measurements. We therefore attribute the hysteresis in χ - H below H_p to the inability of the system to fully relax in the hexatic and the Bragg glass state due to random pinning, rather than supercooling of the disordered VL below the thermodynamic critical field, as expected for a first order phase transition.

We can also speculate on why the VL in a 3-D superconductor could follow the same route to disordering as expected for a 2-D system. Since STS images are taken on the surface of the superconductor, the first possibility is that the order-disorder transition observed in our experiment is essentially a surface phenomenon, involving the tip of the vortex lines on the surface of the superconductor. However, this possibility is ruled out, since we observe excellent correspondence between STS and ac χ measurements, where the latter measures the bulk response of the VL. The more likely possibility is that the vortices in our system are

very rigid, with very little bending along the length of the vortices, such that the VL can be visualised as collection of interacting rods all parallel to the magnetic. Since the degree of freedom in the third dimension is quenched in such a situation, the system behaves essentially like a 2D system.

Finally, we can address the issue of whether a vortex liquid is at all realised at low temperatures in a weakly pinned superconductor. At 32 kOe the vortex image starts to get slightly blurred (Fig. 7(a)), with lines of vortices forming a randomly oriented striped pattern. While this suggests that vortices vibrate along these lines, we can still identify all the individual vortices in the STS image. At 34 kOe the motion of the vortices is large enough to form some blurred structures (Fig. 7(b)) signifying the onset of a fluid state. However, a fully fluid vortex liquid state, if at all, is realised in a very narrow range of field close to H_{c2} . At these fields STS measurement does not have enough resolution to convincingly settle this issue.

In summary, the emerging physical picture from our measurements is that the disordering of the VL in a weakly pinned Type II superconductor, happens in two steps: From the Bragg glass state at low field to a hexatic glass, and then from the hexatic glass to an isotropic vortex glass. One unresolved question in the present study whether random pinning is essential to observe the hexatic state. Since theoretically, the possibility of a first-order transition to a disordered state is not precluded in a 2D system, we cannot rule out the possibility that the two-step melting transforms into a single first-order transition below a critical value of disorder. This should be addressed through further experimental and theoretical studies. It would also be interesting to perform similar experiments in systems such as colloidal crystals in random optical traps where the strength of the pinning potential can be continuously tuned by the strength of optical field, which would provide further insight on the role of random pinning on the order-disorder transition.

Methods

Sample preparation

The experiments are performed on an NbSe₂ single crystal ($T_c \sim 5.2$ K) intercalated with 0.75 at. % of Co, grown by iodine vapour transport method. The intercalated Co atoms act as random pinning centres, making the peak effect more pronounced compared to pure NbSe₂ single crystal³³. Stoichiometric amounts of pure Nb, Se and Co, together with iodine as the transport agent were mixed and placed in one end of a quartz tube, which was then evacuated and sealed. The sealed quartz tube was heated up in a two zone furnace for 5 days, with the charge-zone and growth-zone temperatures kept at, 800⁰ C and 720⁰ C respectively. We obtained single crystals of nominal composition Co_{0.0075}NbSe₂ with lateral size of 4-5 mm.

STS measurements

The VL is imaged using a home-built scanning tunneling microscope³⁴ (STM) operating down to 350 mK and fitted with an axial 9 T superconducting solenoid. Prior to STM measurements, the crystal is cleaved in-situ in vacuum, giving atomically smooth facets larger than 1 $\mu\text{m} \times 1 \mu\text{m}$. Since the vortex core behaves like a normal metal, well resolved images of the VL are obtained by measuring the tunneling conductance ($G(V) = dI/dV$) over the surface at a fixed bias voltage ($V \sim 1.2$ mV) close to the superconducting energy gap, such that each vortex core manifests as a local minimum in $G(V)$. The precise position of the vortices are obtained from the images after digitally removing scan lines and finding the local minima in $G(V)$ using WSxM software³⁵. To identify topological defects, we Delaunay triangulate the VL and determine the nearest neighbor coordination for each flux lines. Topological defects in the hexagonal lattice manifest as points with 5-fold or 7-fold coordination number.

-
- ¹G. Blatter, M. V. Feigel'man, V. B. Geshkenbein, A. I. Larkin, and V. M. Vinokur, *Vortices in high-temperature superconductors*, Rev. Mod. Phys. **66**, 1125 (1994).
- ²M. J. Higgins and S. Bhattacharya, *Varieties of dynamics in a disordered flux-line lattice*, Physica C **257**, 232(1996).
- ³Y. Paltiel, E. Zeldov, Y. N. Myasoedov, H. Shtrikman, S. Bhattacharya, M. J. Higgins, Z. L. Xiao, E. Y. Andrei, P. L. Gammel and D. J. Bishop, *Dynamic instabilities and memory effects in vortex matter*, Nature **403**, 398 (2000).
- ⁴E. H. Brandt, *The flux-line lattice in superconductors*, Rep. Prog. Phys. **58**, 1465 (1995).
- ⁵Giamarchi, T. & Le Doussal, P. Elastic theory of flux lattices in the presence of weak disorder. Phys. Rev. B **52**, 1242 (1995).
- ⁶Fisher, D. S., Fisher, M. P. A., & Huse, D. A. Thermal Quenches, quenched disorder, phase transitions, and transport in type-II superconductors. Phys. Rev. B **43**, 130 (1991).
- ⁷W. Henderson, E. Y. Andrei, M. J. Higgins and S. Bhattacharya, *Metastability and Glassy Behavior of a Driven Flux-Line Lattice*, Phys. Rev. Lett. **77**, 2077 (1996).
- ⁸G. Pasquini, D. Pérez Daroca, C. Chliotte, G. S. Lozano and V. Bekeris, *Ordered, Disordered, and Coexistent Stable Vortex Lattices in NbSe₂ Single Crystals*, Phys. Rev. Lett. **100**, 247003 (2008).
- ⁹J. M. Kosterlitz and D. J. Thouless, *Early work on Defect Driven Phase Transitions*, in 40 years of Berezinskii-Kosterlitz-Thouless Theory, ed. Jorge V Jose (World Scientific, 2013).
- ¹⁰V. Berezinskii, *Destruction of long-range order in one-dimensional and two-dimensional systems possessing a continuous symmetry group. II. Quantum systems*, Sov. Phys. JETP **34**, 610 (1972).
- ¹¹J. M. Kosterlitz and D. J. Thouless, *Ordering, metastability and phase transitions in two-dimensional systems*, J. Phys. C **6**, 1181 (1973).
- ¹²B. I. Halperin, and D. R. Nelson, *Theory of two-dimensional melting*, Phys. Rev. Lett. **41**, 121 (1978).
- ¹³A. P. Young, *Dislocation-mediated melting in two dimensions*, Phys. Rev. B **19**, 2457 (1979).
- ¹⁴J. M. Kosterlitz and D. J. Thouless, *Early work on Defect Driven Phase Transitions*, in 40 years of Berezinskii-Kosterlitz-Thouless Theory, ed. Jorge V Jose (World Scientific, 2013).
- ¹⁵P. Berghuis, A. L. F. van der Slot, and P. H. Kes, *Dislocation-mediated vortex-lattice melting in thin films of a-Nb₃Ge*, Phys. Rev. Lett. **65**, 2583 (1990).

-
- ¹⁶A. Yazdani, W. R. White, M. R. Hahn, M. Gabay, M. R. Beasley, and A. Kapitulnik, *Observation of Kosterlitz–Thouless-type melting of the disordered vortex lattice in thin films of alpha-MoGe*, Phys. Rev. Lett. **70**, 505 (1993).
- ¹⁷I. Guillamón, H. Suderow, A. Fernández-Pacheco, J. Sesé, R. Córdoba, J. M. De Teresa, M. R. Ibarra and S. Vieira, *Direct observation of melting in a two-dimensional superconducting vortex lattice*, Nat. Phys. **5**, 651 (2009).
- ¹⁸Mohan, S., Sinha, J., Banerjee, S. S., Sood, A. K., Ramakrishnan, S., & Grover, A. K. *Large Low-Frequency Fluctuations in the Velocity of a Driven Vortex Lattice in a Single Crystal of 2H-NbSe₂ Superconductor*, Phys. Rev. Lett. **103**, 167001 (2009).
- ¹⁹K. Ghosh, S. Ramakrishnan, A. K. Grover, G. I. Menon, G. Chandra, T. V. Chandrasekhar Rao, G. Ravikumar, P. K. Mishra, V. C. Sahni, C. V. Tomy, G. Balakrishnan, D. Mck Paul and S. Bhattacharya, *Reentrant Peak Effect and Melting of a Flux Line Lattice in 2H-NbSe₂*, Phys. Rev. Lett. **76**, 4600 (1996).
- ²⁰Banerjee, S. S., Patil, N. G., Ramakrishnan, S., Grover, A. K., Bhattacharya, S., Ravikumar, G., Mishra, P. K., Chandrasekhar Rao, T. V., Sahni, V. C. & Higgins, M. J. *Metastability and switching in the vortex state of 2H-NbSe₂*, Appl. Phys. Lett. **74**, 126 (1999).
- ²¹Ravikumar, G., Sahni, V. C., Grover, A. K., Ramakrishnan, S., Gammel, P. L., Bishop, D. J., Bucher, E., Higgins, M. J., & Bhattacharya, S. *Stable and metastable vortex states and the first-order transition across the peak-effect region in weakly pinned 2H-NbSe₂*, Phys. Rev. B **63**, 024505 (2000).
- ²²Pastoriza, H., Goffman, M. F., Arribére, A., & de la Cruz, F. *First Order Phase Transition at the Irreversibility Line of Bi₂Sr₂CaCu₂O_{8+δ}*, Phys. Rev. Lett. **72**, 2951 (1994).
- ²³A. A. Larkin and Y. Ovchinnikov, *Pinning in type II superconductors*, J. Low Temp. Phys. **34**, 409 (1979).
- ²⁴G. D'Anna, M.-O. André, W. Benoit, E. Rodríguez, D.S. Rodríguez, J. Luzuriaga and J.V. Wasczak, *Flux-line response in 2H-NbSe₂ investigated by means of the vibrating superconductor method*, Physica C **218**, 238 (1993).
- ²⁵G. I. Menon and C. Dasgupta, *Effects of pinning disorder on the correlations and freezing of the flux liquid in layered superconductors*, Phys. Rev. Lett. **73**, 1023 (1994)
- ²⁶S. Sengupta, C. Dasgupta, H. R. Krishnamurthy, G. I. Menon, and T. V. Ramakrishnan, *Freezing of the vortex liquid in high-T_c superconductors: A density-functional approach*, Phys. Rev. Lett. **67**, 3444 (1991).

-
- ²⁷Y. Paltiel, E. Zeldov, Y. Myasoedov, M. L. Rappaport, G. Jung, S. Bhattacharya, M. J. Higgins, Z. L. Xiao, E. Y. Andrei, P. L. Gammel, and D. J. Bishop, *Instabilities and Disorder-Driven First-Order Transition of the Vortex Lattice*, Phys. Rev. Lett. **85**, 3712 (2000).
- ²⁸J. Kierfeld and V. Vinokur, *Lindemann criterion and vortex lattice phase transitions in type-II superconductors*, Phys. RevB **69**, 024501 (2004).
- ²⁹S. B. Roy, P. Chaddah, and S. Chaudhary, *Peak effect in CeRu₂: History dependence and supercooling*, Phys. Rev. B **62**, 9191 (2000).
- ³⁰A. P. Petrović, Y. Fasano, R. Lortz, C. Senatore, A. Demuer, A. B. Antunes, A. Paré, D. Salloum, P. Gougeon, M. Potel and Ø. Fischer, *Real-Space Vortex Glass Imaging and the Vortex Phase Diagram of SnMo₆S₈*, Phys. Rev. Lett. **103**, 257001 (2009).
- ³¹A. M. Troyanovski, M. van Hecke, N. Saha, J. Aarts and P. H. Kes, *STM Imaging of Flux Line Arrangements in the Peak Effect Regime*, Phys. Rev. Lett. **89**, 147006 (2002).
- ³²M. Marchevsky, M. J. Higgins and S. Bhattacharya, *Two coexisting vortex phases in the peak effect regime in a superconductor*, Nature **409**, 591 (2001).
- ³³M. Iavarone, R. Di Capua, G. Karapetrov, A. E. Koshelev, D. Rosenmann, H. Claus, C. D. Malliakas, M. G. Kanatzidis, T. Nishizaki, and N. Kobayashi, *Effect of magnetic impurities on the vortex lattice properties in NbSe₂ single crystals*, Phys. Rev. B **78**, 174518 (2008).
- ³⁴A. Kamlapure, G. Saraswat, S. C. Ganguli, V. Bagwe, P. Raychaudhuri, and S. P. Pai, *A 350 mK, 9 T scanning tunneling microscope for the study of superconducting thin films on insulating substrates and single crystals*, Rev. Sci. Instrum. **84**, 123905 (2013).
- ³⁵I. Horcas, R. Fernández, J. M. Gómez-Rodríguez, J. Colchero, J. Gómez-Herrero, and A. M. Baro, *WSXM: A software for scanning probe microscopy and a tool for nanotechnology*, Rev. Sci. Instrum. **78**, 013705 (2007).

Acknowledgements

We thank Shobo Bhattacharya, Rajdeep Sensarma and Deepak Dhar for valuable discussions during the course of this work.

Author Contributions

SCG performed the STS measurements. SCG and GS analysed the STS data. RG and HS performed the bulk pinning measurements and analysed the data. PR conceptualised the problem, supervised the measurements and analysis and wrote the paper. PS and VB carried out growth and characterisation of the samples in collaboration with AT. All authors discussed the results and commented on the manuscript.

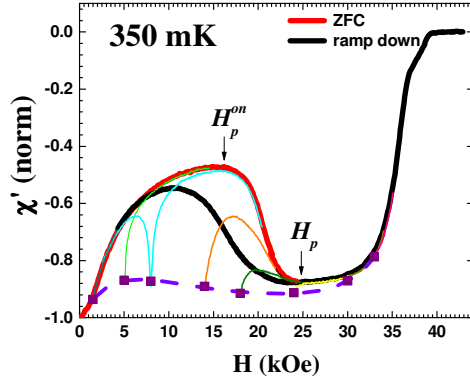


Figure 1. Magnetic field (H) dependence of the ac susceptibility (χ') at 350 mK for the VL prepared using different thermomagnetic cycling. The red line is χ' - H when the magnetic field is slowly ramped up after cooling the sample in zero field (ZFC state). The black line is χ' - H when the magnetic field is ramped down from a value higher than H_{c2} . The square symbols stand for the χ' for the FC states obtained by cooling the sample from $T > T_c$ in the corresponding field; the dashed line shows the locus of these FC states created at different H . The thin lines starting from the square symbols show the evolution of χ' when the magnetic field is ramped up or ramped down (ramped down segment shown only for 0.8 T), after preparing the VL in the FC state. We observe that the FC state is extremely unstable to any perturbation in magnetic field. χ' is normalised to the zero field value for the ZFC state.

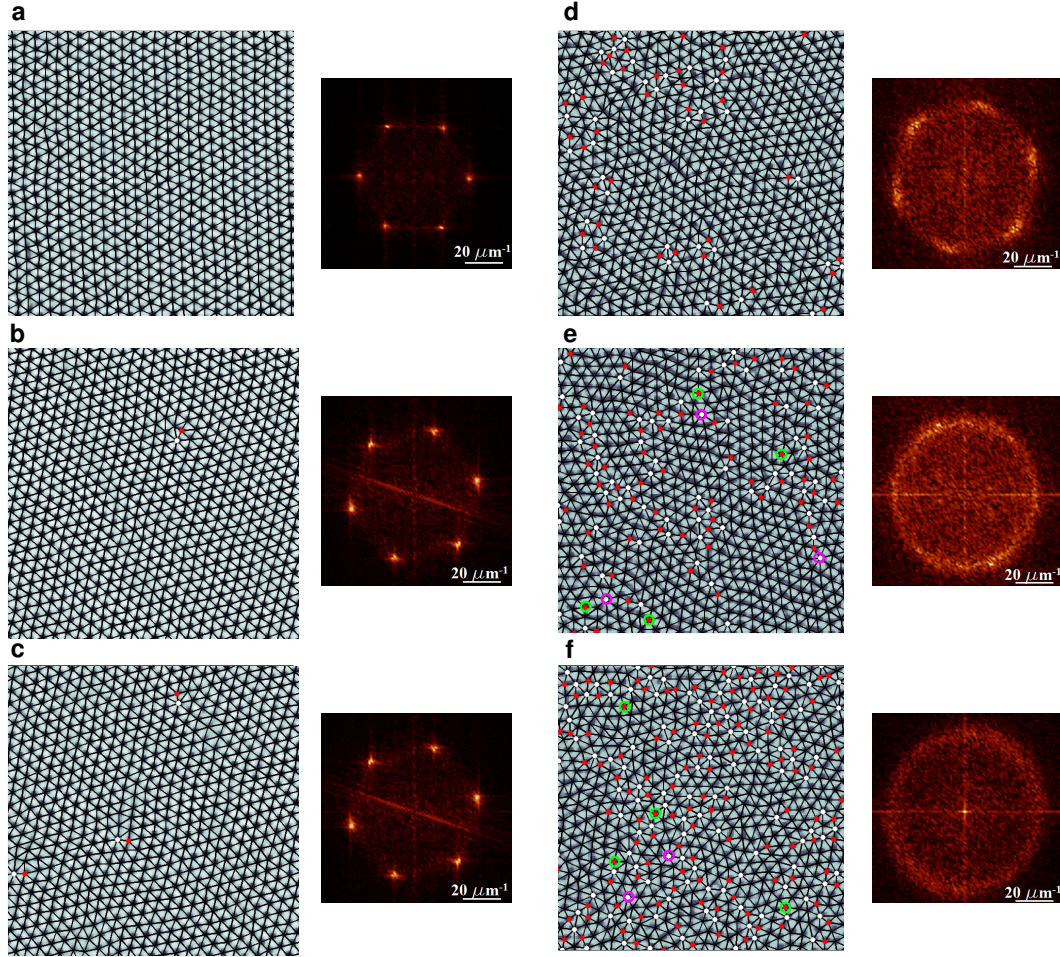


Figure 2. Real space ZFC vortex lattice image along with their Fourier transforms. The magnetic fields are (a) 1.5 T, (b) 2T, (c) 2.4 T, (d) 2.5 T, (e) 2.6 T and (f) 3 T. Delaunay triangulation of the VL are shown as solid lines joining the vortices and sites with 5-fold and 7-fold coordination are shown as red and white dots respectively. The disinclinations (unpaired 5-fold or 7-fold coordination sites) observed at 2.6 and 3 T are highlighted with green and purple circles. While all images are acquired over $1\text{ }\mu\text{m} \times 1\text{ }\mu\text{m}$ area, images shown here have been zoomed to show around 600 vortices for clarity.

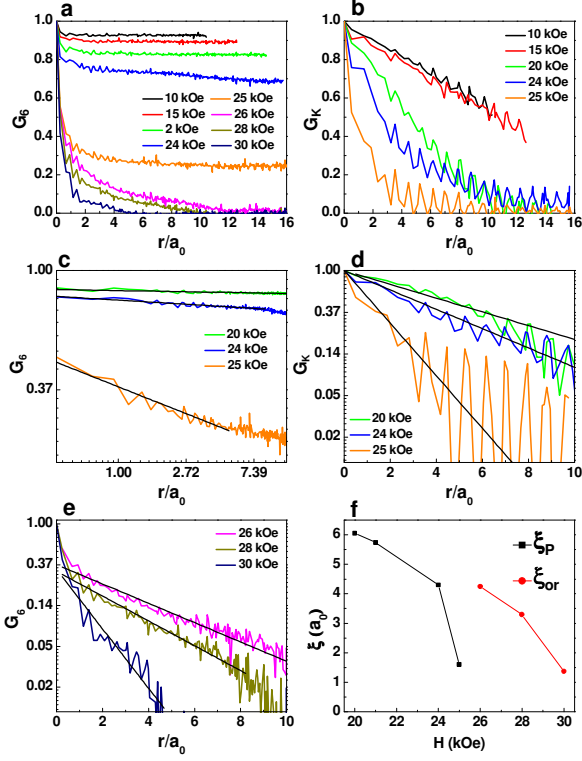


Figure 3. (a) Orientational correlation function, G_6 and (b) and positional correlation function, G_k (averaged over the principal symmetry directions) as a function of r/a_0 for the ZFC state at various fields. a_0 is calculated by averaging over all the bonds after Delaunay triangulating the image. (c) G_6 plotted in log-log scale and (d) G_k plotted in semi-log scale for 20 kOe, 24 kOe and 25 kOe, showing the power law decay of G_6 and exponential decay of G_k , corresponding to a hexatic glass. (e) G_6 plotted in semi-log scale for 26 kOe, 28 kOe, 30 kOe showing exponential decay of G_6 corresponding to a vortex glass state. The solid lines in (c)-(e) are fits to the power-law/exponential decay. (f) Characteristic decay lengths in units of a_0 extracted from the fits for the positional order (ξ_p) in the hexatic state and the orientational order (ξ_{or}) in the vortex glass state respectively.

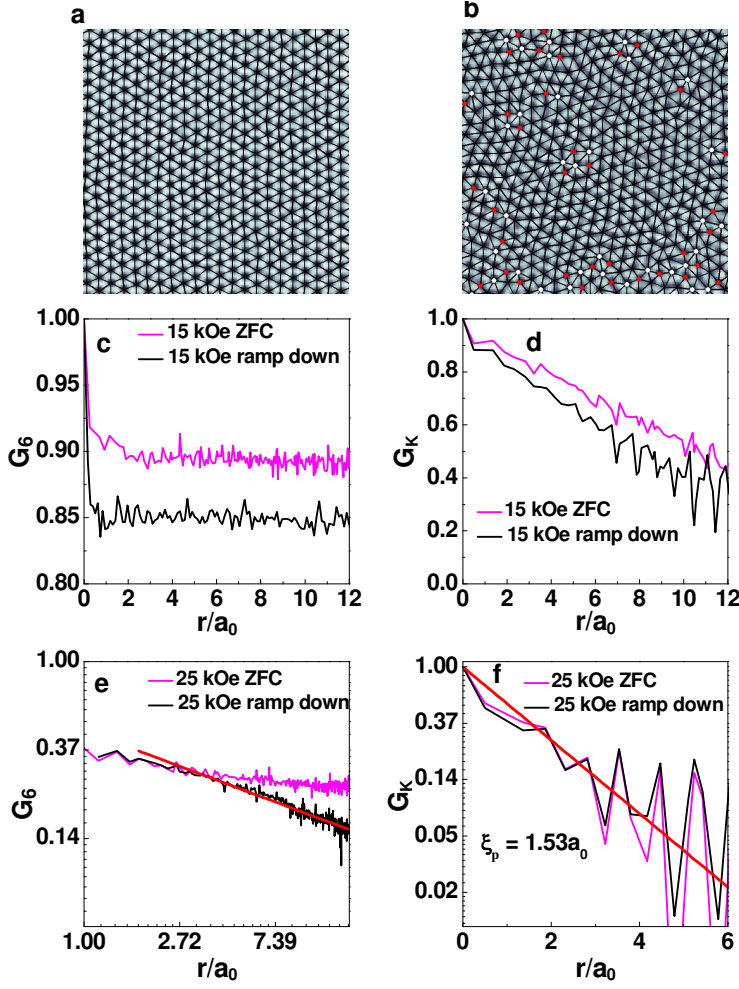


Figure 4. VL image at 350 mK at (a) 15 kOe and (b) 25 kOe when the magnetic field is ramped down from $H > H_{c2}$. Spatial variation of G_6 and G_k (black lines) at (c)-(d) 15 kOe and (e)-(f) 25 kOe respectively. (e) is plotted in log-log scale and (f) is plotted in semi-log scale; the red lines are fits to the power-law and exponential decay respectively. For comparison, G_6 and G_k for the ZFC state (purple lines) are also shown in the same figures. Real space images are zoomed to show ~ 450 vortices for clarity.

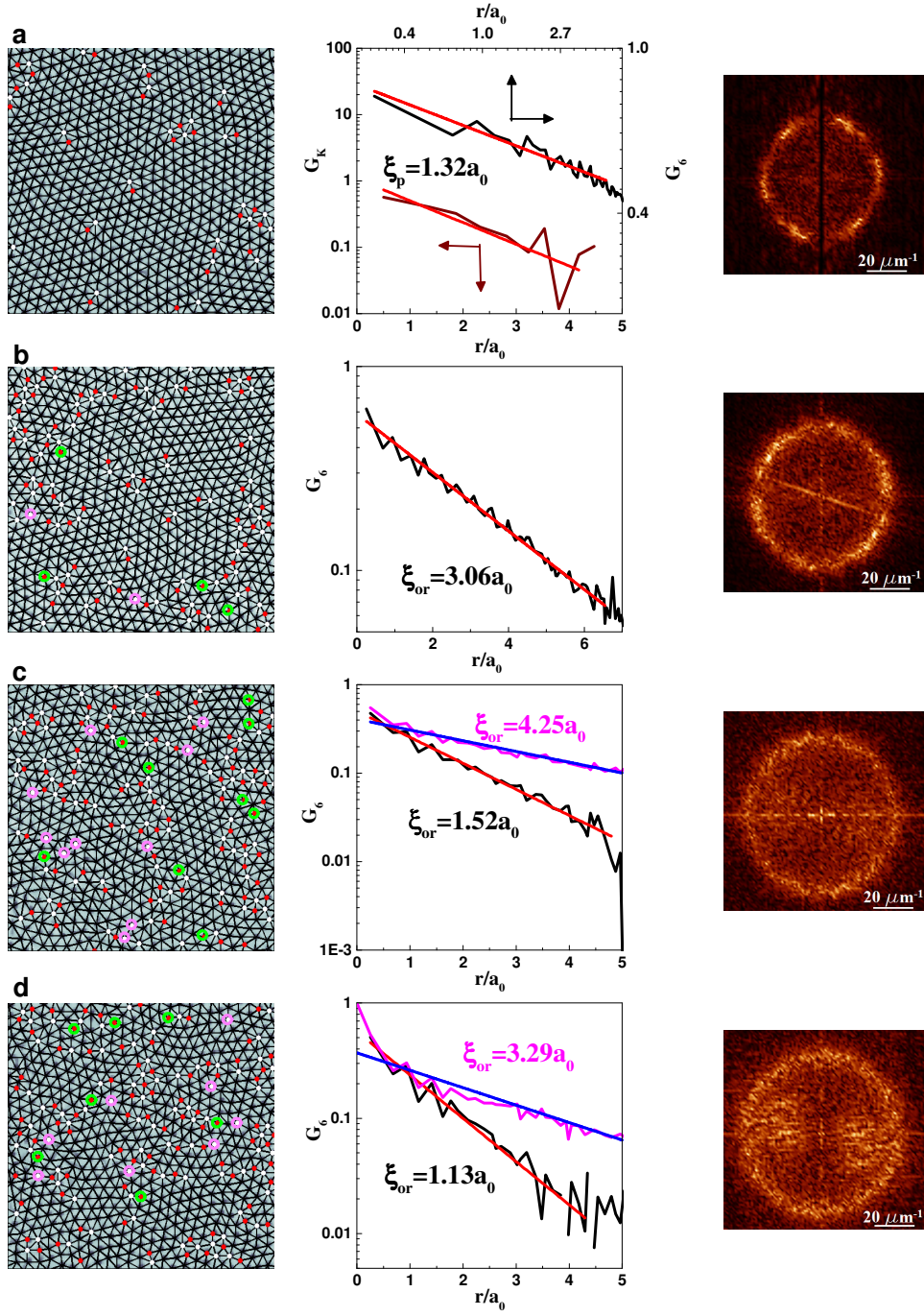


Figure 5. Field Cooled VL images (left column) along with the correlation functions (middle column) and the Fourier transform of the images (right column) at different fields: (a) 1.5 T (b) 2 T (c) 2.6 T (d) 2.8 T. Delaunay triangulation of the VL are shown as solid lines joining the vortices and sites with 5-fold and 7-fold coordination are shown as red and white dots respectively. The disinclinations are highlighted with green and purple circles.

In panel (a) G_6 (black line) is plotted in log-log scale, and G_k (brown line) is plotted in semi-log scale to highlight the power-law and exponential decay respectively. In panels (b)-(d) G_6 is plotted in semi-log scale (black line) to show the exponential decay. The red straight lines passing through the data are the fits to the exponential/power-law behaviour and ξ_p and ξ_{or} extracted from the fits are shown in the respective panels. In panels (c) and (d) the variation of G_6 for the ZFC state (purple line) along with the fits for exponential decay (blue line) at the same magnetic field is shown for comparison. While all images are acquired over $1\text{ }\mu\text{m} \times 1\text{ }\mu\text{m}$ area, images shown here have been zoomed to show around 600 vortices for clarity.

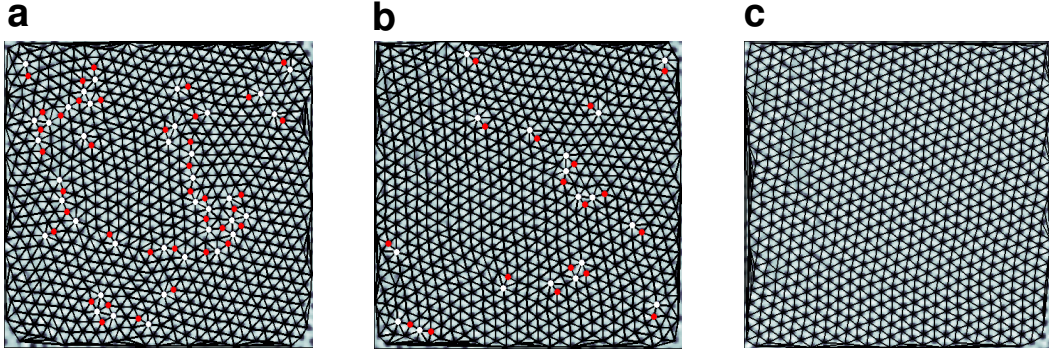


Figure 6. Annihilation of dislocations in a FC vortex lattice at 15 kOe with application magnetic field pulse. (a) FC VL at 350 mK; the same VL after a applying a magnetic field pulse of (b) 0.3 kOe and (c) 0.9 kOe. Dislocations in the VL are shown as pairs of adjacent points with five-fold (red) and seven-fold (white) coordination. In (b) many of the dislocations are annihilated, whereas in (c) all dislocations are annihilated.

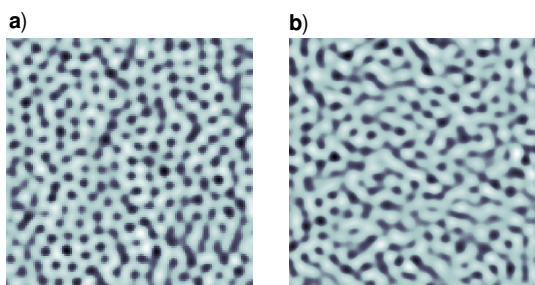


Figure 7. VL images ($400\text{ nm} \times 400\text{ nm}$) at 350 mK at (a) 32 kOe and (b) 34 kOe .